

**DSCC2010-4013**

**THE REVERSE SIGMOID CA-PTH RELATIONSHIP IS NOT SYMMETRICAL**

**Rajiv P. Shrestha\***

Department of Mechanical and Industrial Engineering  
University of Massachusetts  
Amherst, Massachusetts 01003, USA  
Email: rshresth@engin.umass.edu

**Christopher V. Hollo**

Department of Electrical and Computer Engineering  
University of Massachusetts  
Amherst, Massachusetts 01003, USA

**Yossi Chait**

Department of Mechanical and Industrial Engineering  
University of Massachusetts  
Amherst, Massachusetts 01003, USA

**Claus P. Schmitt**

Division of Pediatric Nephrology  
University of Heidelberg  
69120 Heidelberg, Germany

**Stuart R. Chipkin**

Department of Kinesiology  
University of Massachusetts  
Amherst, Massachusetts 01003, USA

**ABSTRACT**

*We present a new, two-pool, linear, time-varying model to describe the short term dynamics of the Ca-PTH axis. We use an asymmetrical reverse sigmoid PTH secretion rate function in the model. This results in an asymmetrical reverse sigmoid relationship between plasma  $Ca^{++}$  and plasma parathyroid hormone (PTH) concentrations (Ca-PTH relationship). In the first validation of this kind, with parameters estimated separately based on each subject's hypocalcemic clamp test data, we successfully test the model's ability to predict the same subject's induced hypercalcemic clamp test responses. We then show that the conventional symmetrical reverse sigmoid Ca-PTH relationship is deficient.*

**1 INTRODUCTION**

In humans, a decrease in plasma  $Ca^{++}$  concentration acutely stimulates PTH secretion by exocytosis of PTH stored in the se-

cretory granules of the parathyroid cells in a time-scale of minutes [1]. Conversely, a rise in the plasma  $Ca^{++}$  concentration inhibits this secretion. This acute stimulation and inhibition of PTH secretion in the parathyroid gland (PTG) is mediated by calcium sensing receptors present in the chief cells of the parathyroid gland. We refer to this system as the Ca-PTH axis. The Ca-PTH axis is an important, and an intricate, subsystem of calcium homeostasis.

Calcium homeostasis refers to a complex bio-mechanism that regulates plasma ionized calcium ( $Ca^{++}$ ) concentration in the human body, within a narrow range, crucial for maintaining normal physiology and metabolism. The overall calcium homeostatic system consists of several subsystems, which operate at different time-scales ranging from minutes to weeks. These subsystems affect pools of  $Ca^{++}$  in compartments related to plasma, bone, kidney, and intestine. A perturbation in one subsystem affects the interconnected subsystems and these in turn affect other subsystems. These cascade effects propagate in positive and negative feedback pathways in multiple directions.

---

\*Address all correspondence to this author.

The response of the Ca-PTH axis to acute changes in the plasma  $\text{Ca}^{++}$  concentration occurs in the time-scales of seconds to minutes [1]. This response is much faster than time scales of other pathways in the calcium homeostatic system that operate in the time-scales of hours to days [2–4]. It is therefore plausible and feasible to analyze the acute response of the Ca-PTH axis separately from the overall system. In this context, we develop a new, two-pool, linear, time-varying model to describe the Ca-PTH axis using an asymmetrical reverse sigmoid Ca-PTH relationship. The parameters of our model are estimated based on hypocalcemic clamp test data obtained from healthy subjects. This model with parameters estimated separately for each subject’s hypocalcemic clamp test responses was validated successfully by testing the model’s ability to predict the same subject’s induced hypercalcemic clamp test response. We then show that if the conventional symmetrical reverse sigmoid Ca-PTH relationship, which has been the cornerstone of Ca-PTH models, is used instead of the asymmetrical relationship, the model is not able to predict a subject’s induced hypercalcemic clamp test response. This shows that the reverse sigmoid Ca-PTH relationship is not symmetrical.

This paper is organized as follows. Section 2 reviews existing models for calcium homeostasis and Ca-PTH axis. Section 3 presents the new mathematical model for the acute Ca-PTH axis. Section 4 describes the estimation of model parameters based on hypocalcemic clamp test, followed by the model prediction results of hypercalcemic clamp test in Section 5. Section 6 contains a discussion followed by conclusions in Section 7.

## 2 A REVIEW OF EXISTING MODELS

The application of a four-parameter logistic model to describe the reverse sigmoid-shaped response pattern [5] has existed for years; A key contribution to calcium homeostasis modeling has been the utilization of such a relationship between PTH secretion rate and plasma  $\text{Ca}^{++}$  steady-state concentrations in [6]. This model, illustrated in Figure 1, is described by

$$\text{PTH secretion rate} = \frac{A - B}{1 + \left(\frac{Ca}{S}\right)^m} + B,$$

where  $A$  and  $B$  denote maximal and minimal values of the secretion rate, respectively,  $Ca$  denotes plasma  $\text{Ca}^{++}$  concentration,  $S$  is the value of  $Ca$  when the PTH secretion rate =  $\frac{A+B}{2}$ , and  $m = \tan(\theta)$  is the slope of the curve at  $S$ . We call this a symmetrical reverse sigmoid relationship, because the absolute rate of change of the slope of the curve for  $Ca < S$  by a small amount is the same as the absolute rate of change of the slope of the curve for  $Ca > S$  by the same amount. A symmetrical reverse sigmoid Ca-PTH relationship has been used to relate PTH secretion rate to the extracellular  $\text{Ca}^{++}$  concentrations in parathyroid

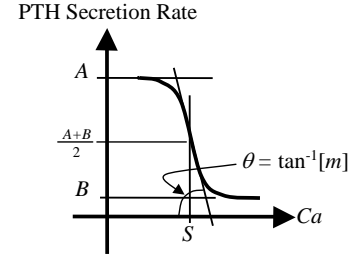


FIGURE 1. The reverse sigmoid curve.

cell cultures prepared from normal bovine, normal human, and pathological human parathyroid tissues in vitro [6]. While some researchers utilized this original form [7–10] other researchers modified it to relate plasma PTH concentration to  $\text{Ca}^{++}$  concentration [11–18]. The Ca-PTH curve has been suggested as a possible bio-tool for assessing health and disease states associated with calcium homeostasis [19]. We show in the paper that the symmetric nature of the curve has limited utility in modeling the dynamics of Ca-PTH axis.

The first attempt to model the short time-scale dynamics (in minutes) in the Ca-PTH axis utilized two PTH pools, one in the parathyroid cells and the other in the blood [20]. By assuming a step change in calcium, the resulting Ca-PTH dynamics was simplified into a linear, time-invariant model. A relatively recent attempt to model plasma calcium homeostasis consisted of pools of calcium, phosphate, PTH, calcitriol in plasma, intracellular phosphate, and parathyroid gland mass [21]. Exchangeable pools of calcium and phosphate in the bone were introduced to model flux exchange between plasma and bone, a renal  $1,\alpha$  hydroxylase, a phosphate pool, and an intestinal calcium pool were included to capture the dynamics involving the kidney and the intestine. The authors estimated model parameters from published clinical experiments involving acute changes in the plasma  $\text{Ca}^{++}$  concentrations. Limited details, however, were offered on how the large number of unknown parameters in this complicated model were estimated. To the best of our knowledge, all published papers in this area have focused only on model parameter estimation and none have reported prediction results, an important component of model validation.

## 3 CA-PTH MODEL

The basic model comprises two pools of PTH, one in the PTG and the other in the plasma as shown in Figure 2. In response to an acute decrease (time-scale of minutes) in the plasma  $\text{Ca}^{++}$  concentration, signal transduction pathways involving the calcium receptors on the parathyroid chief cells in the PTG stimulate exocytosis of the PTH stored in the vesicles of the cells. Conversely, a rise in the plasma  $\text{Ca}^{++}$  concentration inhibits exocytosis of PTH; PTH response occurs on a times-scale of min-

utes [22]. Note that we assume that the parathyroid gland can be modeled as an aggregate of homogenous active chief cells.

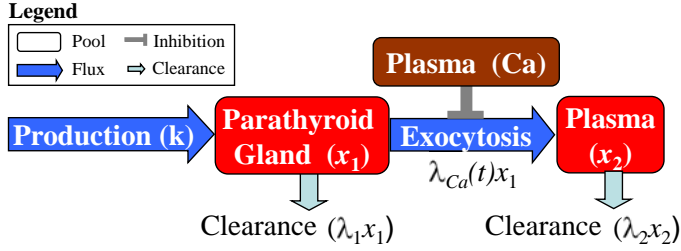


**FIGURE 2.** The Ca-PTH axis.

Using mass balance, the rate of change of PTH in the PTG pool is given by

$$\dot{x}_1(t) = \underbrace{k(t)}_{\text{PTH production}} - \underbrace{\lambda_{Ca}(t)x_1(t)}_{\text{Secretion to plasma}} - \underbrace{\lambda_1 x_1(t)}_{\text{Decay}}, \quad (1)$$

where  $x_1(t)$  denotes the total amount of PTH in the PTG pool,  $k(t)$  denotes the production rate of PTH in the PTG pool,  $\lambda_1$  denotes the decay rate constant of PTH inside the parathyroid cells, and  $\lambda_{Ca}(t)$  denotes the secretion rate function [20]. Since we are considering the response in time scale of minutes, it is reasonable to assume that the synthesis rate of PTH is constant because the regulation of PTH synthesis in response to changes in the plasma  $Ca^{++}$  concentration occurs in time-scale of hours to days [3, 23, 24]. Thus, from here on we set  $k(t)=k$ .

In preliminary studies, we have discovered that if a model, based on hypocalcemic test data, with a conventional symmetric reverse sigmoid secretion function is used, the resulting model cannot predict hypercalcemia PTH response in the same subject. This led us to conclude that one ought to allow for non-symmetrical sensitivity (i.e., slope) across the set point (in Section 6 we demonstrate the limitation of the symmetric curve in terms of the fitted model's ability to predict hypo- or hypercalcemic test results). To this end, we propose an asymmetrical reverse sigmoid secretion rate function

$$\lambda_{Ca}(t) = \frac{A-B}{1 + \left(\frac{Ca(t)}{S}\right)^{m(Ca)}} + B, \quad (2)$$

where the slope or the sensitivity of the secretion rate function is determined by  $m(Ca)$  described by the logistic equation<sup>1</sup>

$$m(Ca) = \frac{m_1}{1 + e^{-\beta(R-Ca(t))}} + m_2, \quad (3)$$

and where (sufficiently large)  $\beta$  forces  $m$  to sharply switch from  $m_2$  to  $m_1 + m_2$  as calcium level decreases below the offset value

<sup>1</sup>Note that the logistic equation has a history of use in statistical analysis of biological assay, for example, see [25].

$R$ . The curve (2) can be viewed as a combination of a low sensitivity curve at calcium levels below  $R$ , and a high sensitivity curve at calcium levels above  $R$ , as illustrated in Figure 3. The role of  $R$  is to modify the range of lower sensitivity curve in the overall asymmetrical reverse sigmoid curve. We would like to emphasize that the biological and physiological explanation of this asymmetrical Ca-PTH relationship requires further exploration.

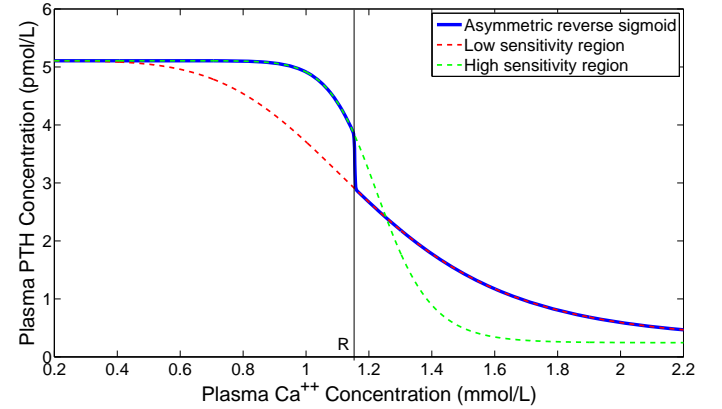


**FIGURE 3.** An asymmetrical reverse sigmoid curve.

Proceeding to the second pool, the rate of change of PTH in the plasma pool is given by a mass balance relation

$$\dot{x}_2(t) = \underbrace{\lambda_{Ca}(t)x_1(t)}_{\text{Secretion from parathyroid glands to plasma}} - \underbrace{\lambda_2 x_2(t)}_{\text{Clearance}}, \quad (4)$$

where  $x_2(t)$  denotes the amount of PTH in the plasma pool and  $\lambda_2$  denotes the biological clearance rate constant for PTH in circulation. The concentration of PTH in circulation,  $[x_2]$ , equals  $x_2(t)$  divided by the average plasma volume of 2.75 liters [26].

There are ten unknown parameters,  $k$ ,  $\lambda_1$ ,  $\lambda_2$ ,  $A$ ,  $B$ ,  $S$ ,  $R$ ,  $m_1$ ,  $m_2$ , and  $\beta$  that completely define the model (1)-(4). We use steady-state relations, along with physiologically relevant quantities, to obtain parameter constraints, to assign initial guesses and the upper and lower bounds, for the parameters during parameter estimation. At steady state, (1) can be written as

$$k = \left[ \frac{A-B}{1 + \left(\frac{\bar{Ca}}{S}\right)^{m(\bar{Ca})}} + B \right] \bar{x}_1 + \lambda_1 \bar{x}_1, \quad m(\bar{Ca}) = \frac{m_1}{1 + e^{-\beta(R-\bar{Ca})}} + m_2, \quad (5)$$

where  $\bar{x}_1$  and  $\bar{Ca}$  denote steady-state levels, respectively. Similarly, (4) can be written as

$$\left[ \frac{A-B}{1 + \left(\frac{\bar{Ca}}{S}\right)^{m(\bar{Ca})}} + B \right] \bar{x}_1 = \lambda_2 \bar{x}_2, \quad m(\bar{Ca}) = \frac{m_1}{1 + e^{-\beta(R-\bar{Ca})}} + m_2, \quad (6)$$

where  $\bar{x}_2$  denotes steady-state level. From (5) and (6) we get  $k = \lambda_2 \bar{x}_2 + \lambda_1 \bar{x}_1$ . Considering the baseline steady-state prior to the initiation of hypocalcemic clamp test, we have

$$k = \lambda_2 \bar{x}_{2,n} + \lambda_1 \bar{x}_{1,n} \quad (7)$$

where  $\bar{x}_{1,n}$  and  $\bar{x}_{2,n}$  denote steady-state baseline PTH amount in the PTG and plasma pool respectively. At extreme values

$$\bar{x}_{1,\max} = \frac{k - \lambda_2 \bar{x}_{2,\min}}{\lambda_1}, \quad \bar{x}_{1,\min} = \frac{k - \lambda_2 \bar{x}_{2,\max}}{\lambda_1}, \quad (8)$$

where  $\bar{x}_{1,\max}$  and  $\bar{x}_{1,\min}$  denote maximum and minimum steady-state values of PTH in the PTG pool, respectively, and  $\bar{x}_{2,\min}$  and  $\bar{x}_{2,\max}$  denote minimum and maximum steady-state values of PTH in the plasma pool, respectively. Evaluating (6) at upper and lower plasma  $\text{Ca}^{++}$  steady-state levels gives

$$\lim_{Ca \rightarrow 0} A \bar{x}_{1,\min} = \lambda_2 \bar{x}_{2,\max} \implies A = \frac{\lambda_2 \bar{x}_{2,\max}}{\bar{x}_{1,\min}} = \frac{\lambda_1 \lambda_2 \bar{x}_{2,\max}}{k - \lambda_2 \bar{x}_{2,\max}}, \quad (9)$$

$$\lim_{Ca \rightarrow \infty} B \bar{x}_{1,\max} = \lambda_2 \bar{x}_{2,\min} \implies B = \frac{\lambda_2 \bar{x}_{2,\min}}{\bar{x}_{1,\max}} = \frac{\lambda_1 \lambda_2 \bar{x}_{2,\min}}{k - \lambda_2 \bar{x}_{2,\min}}. \quad (10)$$

Finally, considering baseline steady-state plasma  $\text{Ca}^{++}$  concentration during hypocalcemic clamp test, the set-point  $S$  can be found from (6).

$$S = Ca_0 \left( -\frac{\bar{x}_{1,n} B - \lambda_2 \bar{x}_{2,n}}{\bar{x}_{1,n} A - \lambda_2 \bar{x}_{2,n}} \right)^{\frac{1}{m(\bar{C}a)}}, \quad m(\bar{C}a) = \frac{m_1}{1 + e^{-\beta(R - \bar{C}a)}} + m_2. \quad (11)$$

Equations (7), (8), (9), and (10) define parameter constraints at steady state.

The model (1)-(4) is a linear, time-varying (LTV) system and it is not possible to derive an analytic solution for the response [2]. One way to simplify the analysis is to assume a step change in calcium [20], which renders  $\lambda_{\text{Ca}}(t)$  a constant, and thus, the system becomes linear, time-invariant. In reality,  $\text{Ca}^{++}$  concentration changes at a much slower rate than a step change and the PTH secretion rate depends on the rate of change of the plasma  $\text{Ca}^{++}$  concentration [27]. Thus, to accurately capture the expected dynamics a model should include a time-varying  $\lambda_{\text{Ca}}(t)$ . Next, we proceed to estimate model parameters based on clinical tests.

#### 4 ESTIMATION OF MODEL PARAMETERS

Model parameters are typically estimated from induced calcemic clamp tests which are also used to study acute changes in the Ca-PTH axis. During an induced hypocalcemic clamp test, plasma  $\text{Ca}^{++}$  concentration is decreased by an intravenous infusion of sodium citrate [22]. During an induced hypercalcemic clamp test, plasma  $\text{Ca}^{++}$  concentration is increased by an intravenous infusion of calcium gluconate [22].

The clinical data we used to estimate the model parameters and validate the model constitutes such hypo- and hypercalcemic

clamp tests. For brevity, we report results only for one subject, referred to as Subject 1 henceforth, and the results corresponding to the other two subjects can be found in [19]. Plasma  $\text{Ca}^{++}$  concentrations were measured every 5 minutes during the induction of hypo- or hypercalcemic clamp and the corresponding plasma PTH concentrations were measured every one minute (see Figures 4- 7). Plasma  $\text{Ca}^{++}$  concentrations were measured less frequently during the baseline period.

In estimating model parameters, we seek to accurately qualify and quantify aspects of the clinical data. Qualitative accuracy is determined by whether the simulation exhibits salient features of clinical PTH responses such as rate of increase or decay, peaking, and steady state behavior. Quantitative accuracy aims for a reasonable estimation of a ‘smoothed’ clinical response, given that our model is a simple, second-order type, and cannot be expected to follow each data point with great accuracy.

We used the Simulink Design Estimation tool in MATLAB [28] to estimate the following profile of the induced hypocalcemic calcium clamp kinetics

$$Ca(t) = \begin{cases} Ca_0, & t < t_0 \\ Ca_0 - Ca_1(1 - e^{-\alpha(t-t_0)}), & t \geq t_0 \end{cases} \quad (12)$$

where  $Ca_0$  was set to the average baseline value prior to clamp initiation. The estimated kinetics values for the clamp data set is shown below where  $t_0$  is the clamp initiation time<sup>2</sup>. The fitted

Subject	Parameter values
1	$Ca_0 = 1.2550, t_0 = 575; Ca_1 = 0.1817; \alpha = 0.0442$

**TABLE 1.** Estimated hypocalcemic clamp test calcium profile parameter values for a subject.

first-order dynamics follows closely the decaying calcium levels; The clinical hypocalcemic calcium clamp kinetics and their estimation (Eqn. (12) and Table 1) for the data set is shown in Figure 4.

We fed the above calcium profile and the model (1)-(4) into Simulink Design Estimation tool in MATLAB [28]. The parameters were estimated using the Levenberg-Marquardt method and the sum of squared errors cost function. The determination of the starting values used during the parameter estimation are detailed in [19]. The starting values for parameter estimation, lower and upper bounds, and the estimated values for the data set is summarized in Table 2.

In general, the optimization software was able to produce a good qualitative and quantitative correlation with clinical PTH

<sup>2</sup>We ran the simulation for a sufficiently long period first (540 minutes here) in order that it reaches steady state prior to calcium clamp initiation.

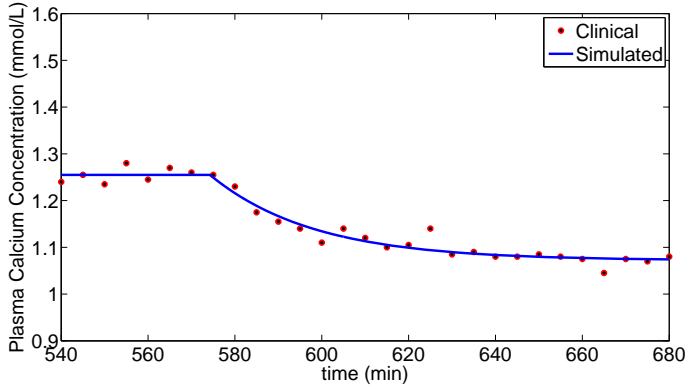


**FIGURE 4.** (Subject 1) Induced hypocalcemic clamp test calcium kinetics: clinical data (dots) and analytical approximation (solid) described by Eqn. (12) and data in Table 1.

	Starting Value	Lower Bound	Upper Bound	Estimated Value	Units
$\lambda_1$	0.01	0	0.1	0.0125	$\text{min}^{-1}$
$\lambda_2$	0.5	.1	$\infty$	0.5595	$\text{min}^{-1}$
$m_1$	100	50	150	112.5200	—
$m_2$	17	15	20	15.0000	—
$R$	1.2050	1	1.2250	1.2162	mmol/L
$\beta$	$10^6$	$10^6$	$10^6$	$10^6$	L/mmol
$\bar{x}_{1,n}$	$100 \times \bar{x}_{2,n}$	100	$\infty$	490.7800	pmol
$\bar{x}_{2,n}$	$2.4372 \times 2.75$	4	12	6.6290	pmol
$\bar{x}_{2,\min}$	0.5	0.1	0.6702	0.6697	pmol
$\bar{x}_{2,\max}$	$5.2815 \times 2.75$	12	20	14.0430	pmol

**TABLE 2.** Initial values, bounds and final estimated model parameters for Subject 1 hypocalcemic calcium clamp test.

concentration response as shown in Figure 5. The simulated response closely tracks the average clinical PTH response, the initial rapid rise that peaks between 5-10 minutes, and the subsequent exponential decay where steady-state PTH level is reached after additional 40-60 minutes. The root mean squared errors<sup>3</sup> for the estimated response is 0.4086.

## 5 PREDICTION RESULTS

The utility of a system model lies in its ability to predict responses observed in data that were not available or used for

<sup>3</sup>Root mean squared error is the square root of the sum of squared residuals divided by the number of data points.

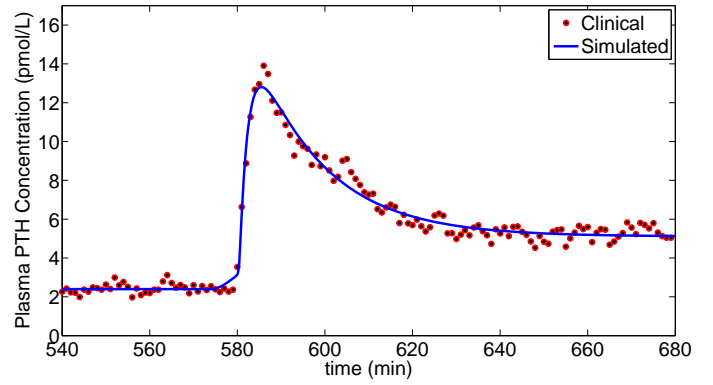


**FIGURE 5.** (Subject 1) PTH,  $x_2(t)/2.75$ , response to induced hypocalcemic clamp test: clinical data (dots) and simulation (solid) using the model (1)-(4) with corresponding estimated parameters in Table 2 and calcium clamp profile in Eqn. (12) and Table 1.

estimation purposes. In Section 3, we described the underlying biological processes of this axis, and in Section 4, we demonstrated that it is feasible to estimate a biologically-relevant set of model parameters using clinical data. This section takes our work to its next logical step – verifying the model’s ability to predict Ca-PTH axis dynamics. We would like to emphasize that the predicted responses described in this section were generated using the model (1)-(4) and parameters in Table 2 that were estimated based on the hypocalcemic clamp test data.

Similar to the calcium profile estimation step carried out for the hypocalcemic clamp test in Section 4, the calcium profile in the induced hypercalcemic clamp test was estimated using the following relation

$$Ca(t) = \begin{cases} Ca_0, & t < t_0 \\ Ca_0 + Ca_1(1 - e^{-\alpha(t-t_0)}), & t \geq t_0 \end{cases} \quad (13)$$

and the corresponding values for the clamp data set is shown below. The fitted first-order dynamics follows closely the increas-

Subject	Parameter values
1	$Ca_0 = 1.2200, t_0 = 575; Ca_1 = 0.2624; \alpha = 0.0569$

**TABLE 3.** Estimated hypercalcemic clamp test calcium profile parameter value.

ing calcium levels; The clinical hypercalcemic calcium clamp kinetics and their estimation for the subject is shown in Figure 6.

The predicted response of PTH concentration,  $x_2(t)/2.75$ , was simulated using the estimated hypercalcemic calcium clamp

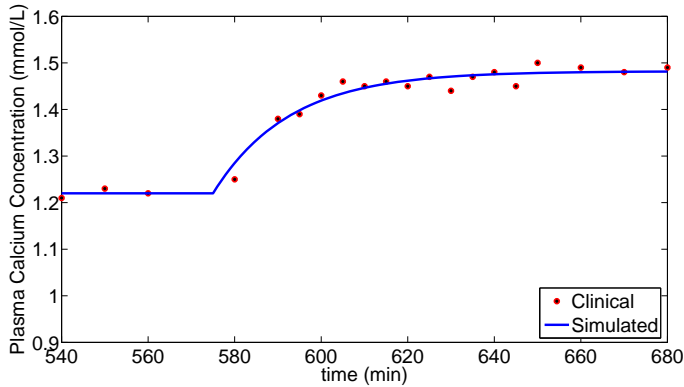


**FIGURE 6.** (Subject 1) Induced hypercalcemic clamp test calcium kinetics: clinical data (dots) and analytical approximation (solid) described by Eqn. (13) and data in Table 3.

kinetics described by Eqn. (13) and Table 3, the model (1)-(4), and parameters in Table 2; Comparisons between clinical and predicted response is shown in Figure 7. We observe a reason-

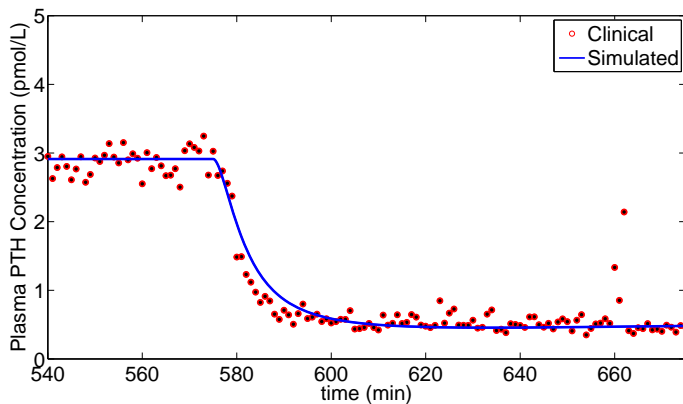


**FIGURE 7.** (Subject 1) Predicted PTH,  $x_2(t)/2.75$ , response to hypercalcemic clamp test: clinical data (dots) and simulation (solid) using the model (1)-(4) with corresponding estimated parameters in Table 2 and calcium clamp profile in Eqn. (13) and Table 1.

ably accurate PTH response prediction. The predicted rate of PTH decay is somewhat slower than observed in data but still within our modeling time frame of minutes. The root mean squared error for the estimated response is 0.1602.

By construction, the secretion rate function  $\lambda_{Ca}(t)$  is an asymmetrical reverse sigmoid. This implies that, at steady state, plasma  $Ca^{++}$  concentration also bears an asymmetrical reverse sigmoid relationship with respect to both plasma PTH concentration and PTH secretion rate from the gland [19]. This relationship is shown in Figure 8.

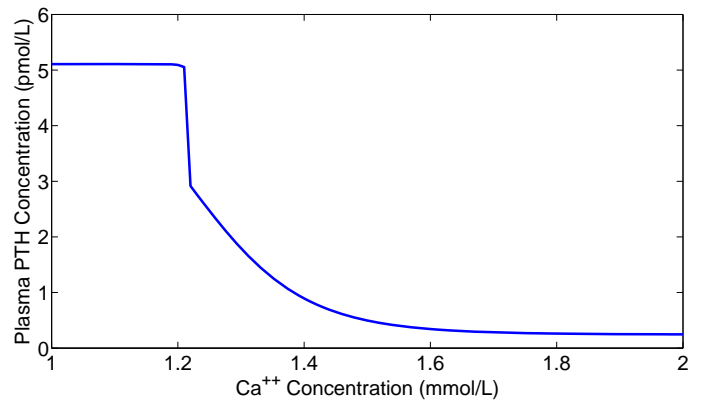


**FIGURE 8.** The asymmetrical reverse-sigmoid relationship between steady-state plasma  $Ca^{++}$  concentration and steady-state plasma PTH concentration for Subject 1.

## 6 DISCUSSION

A salient feature of our Ca-PTH model is the reverse sigmoid Ca-PTH relationship. Using a reverse sigmoid relationship, either symmetrical or asymmetrical, to represent PTH secretion rate from the gland is tantamount to using a single-pool model to describe the dynamics of the Ca-PTH axis [19]. Furthermore, such a single-pool model cannot produce the transient behavior observed in clinical clamp tests [19]. As a result, we have departed from the conventional application of the reverse sigmoid relationship for either PTH secretion rate or PTH concentration relative to plasma  $Ca^{++}$  concentration. Specifically, we introduced a new PTH secretion rate function,  $\lambda_{Ca}(t)$ , a function of plasma  $Ca^{++}$  concentration, that exhibits an asymmetrical reverse sigmoid property, resulting in a time-varying PTH secretion rate  $\lambda_{Ca}(t)x_1$  in (1)-(4).

In addition, we have discovered that the symmetrical form of the reverse sigmoid curve used in applications is of limited utility. To illustrate this point, we present a representative example from an estimation-prediction procedure for Subject 1 that was executed in a similar manner as described in Sections 4-5. To this end, we use the same model described by (1)-(4), however, this time we enforce a symmetrical Ca-PTH relationship by using  $m = \text{constant}$ . In terms of estimating model parameters to match hypocalcemic clamp test data, our experience has shown that a good match can be achieved using either a symmetrical or an asymmetrical Ca-PTH relationship. The match achieved using a symmetrical relationship is shown in Figures 9-10, and is similar to the response (as shown in Figure 5) corresponding to the asymmetrical relationship. The same subject's predicted PTH response shown in Figure 12,  $x_2(t)/2.75$ , to the hypercalcemic clamp (Figure 11) using the symmetrical relationship, however, is qualitatively (e.g., faster) and quantitatively (e.g., large initial value difference) different from the predicted response using the asymmetrical relationship as shown in Figure 7.

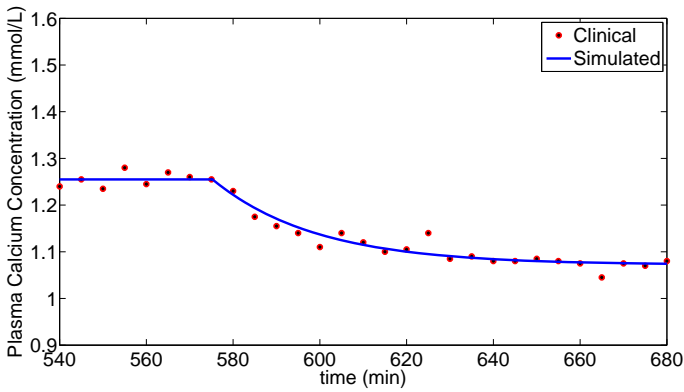


**FIGURE 9.** (Subject 1) Induced hypocalcemic clamp test calcium kinetics: clinical data (dots) and analytical approximation (solid).

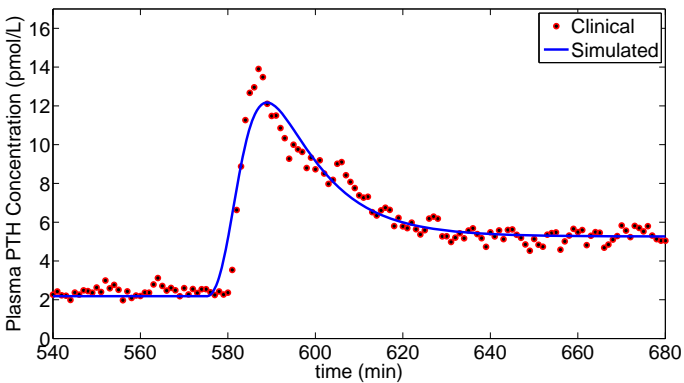


**FIGURE 10.** (Subject 1) Estimated PTH,  $x_2(t)/2.75$ , response to hypocalcemic clamp test: clinical data (dots) and simulation (solid) using symmetric reverse sigmoid PTH secretion function.

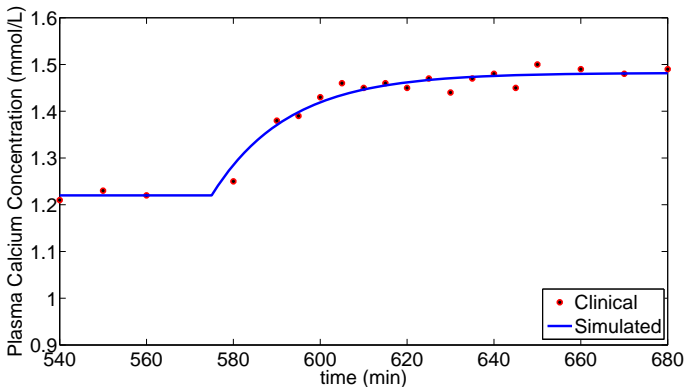


**FIGURE 11.** (Subject 1) Induced hypercalcemic clamp test calcium kinetics: clinical data (dots) and analytical approximation (solid).

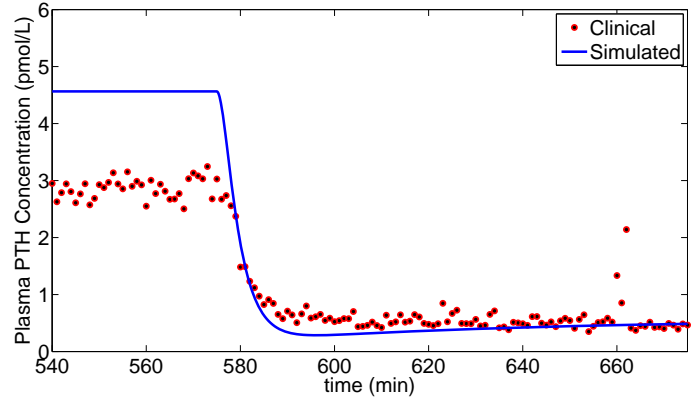


**FIGURE 12.** (Subject 1) Predicted PTH,  $x_2(t)/2.75$ , response to hypercalcemic clamp test: clinical data (dots) and simulation (solid) using symmetric reverse sigmoid PTH secretion function.

These differences appear to suggest that the Ca-PTH axis is more sensitive during severe hypocalcemic conditions than around the normal calcium levels and during hypercalcemia. When model parameters are estimated using hypocalcemic clamp test, a symmetrical Ca-PTH relation will result in an excessively rapid PTH response to hypercalcemic clamp test. Also, small deviations in calcium around normal levels will result in a very large predicted PTH change. Thus, the symmetrical reverse sigmoid Ca-PTH relationship cannot be used to model the Ca-PTH axis and the use of the asymmetrical Ca-PTH relationship is imperative.

## 7 CONCLUSIONS

We developed a new, two-pool, and linear-time-varying model for the acute Ca-PTH axis. We introduced an asymmetric reverse sigmoid PTH secretion rate function which results in an asymmetric reverse sigmoid relationship between steady-state plasma  $\text{Ca}^{++}$  and PTH concentrations. Based on hypocalcemic clamp test data, we estimated the model parameters and successfully validated the model by comparing its prediction with the same subject's hypercalcemic clamp test data. Finally, we motivated the need for an asymmetrical reverse sigmoid Ca-PTH relationship over the conventional symmetrical reverse sigmoid Ca-PTH relationship.

## ACKNOWLEDGMENT

This material is based upon work supported in part by the National Science Foundation (NSF) under Grant No. 0556081. Any opinions, findings and conclusions or recommendations expressed in this material are those of the author(s) and do not necessarily reflect the views of the NSF.

## REFERENCES

- [1] S Yano and EM Brown. *Molecular biology of the parathyroid*, chapter The calcium sensing receptor, pages 44–56. Kluwer Academic/Plenum, New York, 1st edition, 2005.
- [2] RP Shrestha. A Mathematical Model of Acute Response of Parathyroid Hormone to Changes in Plasma Ionized Calcium in Normal Humans. <http://scholarworks.umass.edu/theses/118/>. MS Thesis, University of Massachusetts, Amherst, MA, Jan 2008.
- [3] R Kilav, J Silver, and T Naven-Many. *Molecular biology of the parathyroid*, chapter Regulation of parathyroid hormone mRNA stability by calcium and phosphate, pages 57–67. Kluwer Academic/Plenum Publishers/Landes Bioscience/Eurekah.com, New York, 1st edition, 2005.
- [4] T Naveh-Many and J Silver. *Molecular biology of the parathyroid*, chapter Regulation of parathyroid hormone gene expression by 1,25-dihydroxyvitamin D, pages 84–94. Kluwer Academic/Plenum Publishers, New York, 1st edition, 2005.
- [5] A De Lean, PJ Munson, and D Todbard. Simultaneous analysis of families of sigmoidal curves: application to bioassay, radioligand assay, and physiological dose-response curves. *American Journal of Physiology*, 235(2):E97–E102, 1978.
- [6] EM Brown. Four-parameter model of the sigmoidal relationship between parathyroid hormone release and extracellular calcium concentration in normal and abnormal parathyroid tissue. *Journal of Clinical Endocrinology and Metabolism*, 56:572–581, 1983.
- [7] EM Brown. Extracellular  $\text{Ca}^{2+}$  sensing, regulation of parathyroid cell function, and role of  $\text{Ca}^{2+}$  and other ions as extracellular (first) messengers. *Physiological Reviews*, 71:371–404, 1991.
- [8] EM Brown, RE Wilson, JG Thacher, and SP Marynick. Abnormal calcium-regulated PTH release in normal parathyroid tissue from patients with adenoma. *The American Journal of Medicine*, 71:565–570, 1981.
- [9] EM Brown, RE Wilson, JG Thacher, and SP Marynick. Abnormal regulation of parathyroid hormone release by calcium in secondary hyperparathyroidism due to chronic renal failure. *Journal of Clinical Endocrinology and Metabolism*, 54:172–179, 1982.
- [10] GP Mayer and JG Hurst. Sigmoidal relationship between parathyroid hormone secretion rate and plasma calcium concentration in calves. *Endocrinology*, 102:1036–1042, 1978.
- [11] MJ Borrego, AJ Felsenfeld, A Martin-Malo, Y Almaden, MT Concepcion, P Aljama, and M Rodriguez. Evidence for adaptation of the entire PTH-calcium curve to sustained changes in the serum calcium in hemodialysis patients. *Nephrology Dialysis Transplantation*, 12:505–513, 1997.
- [12] AJ Felsenfeld, M Rodriguez, and E Aguilera-Tejero. Dynamics of parathyroid hormone secretion in health and secondary hyperparathyroidism. *Clin J Am Soc Nephrol*, 2:1283–1305, 2007.
- [13] P D’Amour, A Rakel, JH Brossard, L Rousseau, C Albert, and T Cantor. Acute regulation of circulating parathyroid hormone (PTH) molecular forms by calcium: Utility of pth fragments/PTH (1-84) ratios derived from three generations of PTH assays. *Journal of Clinical Endocrinology and Metabolism*, 91(1):283–289, 2006.
- [14] Moyses RMA, Pereira RC, Reis LMD, Sabbaga E, and Jorgetti V. Dynamic tests of parathyroid hormone secretion using hemodialysis and calcium infusion cannot be compared. *Kidney International*, 5:659–665, 1999.
- [15] V DeCristofaro, C Colturi, A Masa, M Comelli, and LA Pedrini. Rate dependence of acute PTH release and association between basal plasma calcium and set point of calcium-PTH curve in dialysis patients. *Nephrology Dialysis Transplantation*, 16:1214–1221, 2001.
- [16] JA Ramirez, WG Goodman, J Gornbein, C Menezes, L Moulton, GV Segre, and IB Salusky. Direct in vivo comparison of calcium-regulated parathyroid hormone secretion in normal volunteers and patients with secondary hyperparathyroidism. *Journal of clinical endocrinology and Metabolism*, 76:1489–1494, 1993.
- [17] PR Conlin, VT Fajtova, RM Mortensen, MS LeBoff, and EM Brown. Hysteresis in the relationship between serum ionized calcium and intact parathyroid hormone during recovery from induced hyper- and hypocalcemia in normal humans. *Journal of clinical endocrinology and Metabolism*, 69:593–599, 1989.
- [18] CP Schmitt and F Schaefer. Calcium sensitivity of the parathyroid in renal failure: Another look with new method. *Nephrol Dial Transplant*, 14:2815–2818, 1999.
- [19] RP Shrestha, CV Hollo, CP Schmitt, S Chipkin, and Y Chait. A mathematical model of parathyroid hormone response to acute changes in plasma ionized calcium concentration in humans. *Mathematical Biosciences*, In print. doi:10.1016/j.mbs.2010.04.001.
- [20] G Momen and P Schwarz. A mathematical/physiological model of parathyroid hormone secretion in response to blood-ionized calcium lowering in vivo. *Scan J Clin Lab Invest*, 57:381–394, 1997.
- [21] JF Raposo, LG Sobrinho, and HG Ferreira. A minimal mathematical model of calcium homeostasis. *The Journal of Clinical Endocrinology and Metabolism*, 77:4330–4340, 1993.
- [22] CP Schmitt, F Schaefer, A Bruch, JD Vel, H Schmidt-Gayk, G Stein, E Ritz, and O Mehls. Control of pulsatile and tonic parathyroid hormone secretion by ionized calcium. *Journal of Clinical Endocrinology and Metabolism*, 81:4236–4243, 1996.
- [23] JM Brunder, TA Guise, and GR Mundy. *Endocrinology and metabolism*, chapter Mineral metabolism, pages 1079–1177. McGraw-Hill, New York, 4th edition, 2001.
- [24] JF Habener. Regulation of parathyroid hormone secretion and biosynthesis. *Ann. Rev. Physiol.*, 43:211–223, 1981.
- [25] DJ Finney. *Statistical Method in Biological Assay*, chapter Quantal responses and the tolerance distribution, pages 454–455. Hafner Publishing Company, New York, 1st edition, 1952.
- [26] Wikipedia.com. <http://en.wikipedia.org/wiki/Blood>. Blood.
- [27] FD Grant, PR Conlin, and EM Brown. Rate and concentration dependence of parathyroid hormone dynamics during stepwise changes in serum ionized calcium in normal humans. *Journal of Clinical Endocrinology and Metabolism*, 71:370–378, 1990.
- [28] The Mathworks. *Simulink Design Optimization*. Natic, MA, 1.1 edition, 2009.